J Neurophysiol 93: 1920–1934, 2005.
First published November 17, 2004; doi:10.1152/jn.00917.2004.

Integration of Synaptic Responses to Neighboring Whiskers in Rat Barrel Cortex In Vivo

Michael J. Higley and Diego Contreras
Department of Neuroscience, University of Pennsylvania School of Medicine, Philadelphia, Pennsylvania

Submitted 2 September 2004; accepted in final form 15 November 2004

Higley, Michael J. and Diego Contreras. Integration of synaptic responses to neighboring whiskers in rat barrel cortex in vivo. *J Neurophysiol* 93: 1920–1934, 2005. First published November 17, 2004; doi:10.1152/jn.00917.2004. Characterizing input integration at the single-cell level is a critical step to understanding cortical function, particularly when sensory stimuli are represented over wide cortical areas and single cells exhibit large receptive fields. To study synaptic integration of sensory inputs, we made intracellular recordings from the barrel cortex of anesthetized rats in vivo. For each cell, we deflected the principal whisker (PW) either alone or preceded by the deflection of a single adjacent whisker (AW) at an interval of 20 or 3 ms. At the 20-ms interval in all cases, prior AW deflection significantly suppressed the PW-evoked spike output and caused the underlying synaptic response to reach a peak Vm less depolarized than that arising from PW deflection alone. The decrease in peak Vm was not attributed to hyperpolarizing inhibition but to a divisive reduction in PW-evoked PSP amplitude. The reduction in amplitude was not a result of shunting inhibition but was mostly a result of removal of the synaptic drive, or disfacilitation. When the AW–PW interval was shortened to 3 ms, spike suppression was observed in a subset of the cells studied. In most cases, a divisive reduction in synaptic response amplitude was offset by summation with the preceding AW-evoked depolarization. To determine whether suppression is a general feature of synaptic integration by barrel cortex neurons, we also characterized the interaction of responses evoked by local electrical stimulation. In contrast to the whisker data, we found that responses to paired stimulation at the same intervals produced more spikes and reached a peak Vm more depolarized than the individual responses alone, suggesting that whisker-evoked suppression is not a result of postsynaptic mechanisms. Instead, we propose that cross-whisker response suppression depends on sensory-specific mechanisms at cortical and subcortical levels.

INTRODUCTION

Neocortical neurons in vivo are constantly bombarded by synaptic inputs from multiple sources. Characterization of how these inputs are integrated and converted to spike output is a necessary step in understanding the flow of information in neuronal circuits. Synaptic integration depends heavily on the intrinsic properties of single cells. Both passive cable properties and active dendritic conductances shape the interaction of synaptic inputs and regulate the linearity of response integration (Berger et al. 2001; Cash and Yuste 1999; Kuno and Miyahara 1969; Larkum and Zhu 2002; Margulis and Tang 1998; Nettleton and Spain 2000; Schiller et al. 2000; Urban and Barrionuevo 1998). Also critical are the characteristics of the local neuronal circuit, such as recurrent excitation and feedforward and feedback inhibition. The magnitude and temporal pattern of local circuit engagement can influence integration at the single-cell level (Cauller and Connors 1994; Dingledine and Langmoen 1980; Douglas et al. 1995; Koch et al. 1983; Kyriazi and Simons 1993; Langmoen and Andersen 1983; Wilent and Contreras 2004). Here, we use the whisker-barrel system of the rat as an experimental model to study cortical integration of synaptic inputs.

The neural representation of the mystacial vibrissae of the rat is organized into anatomically segregated cytochrome oxidase-rich aggregates of neurons called *barrels* in layer 4 of primary sensory cortex (Welker and Woolsey 1974; Woolsey and Van der Loos 1970). Barrel cells, and the neurons within the same cortical column, are excited most strongly by deflection of a single vibrissa termed the *principal whisker* (PW) (Simons 1978; Welker 1976). Cells within a barrel column are also excited to a lesser degree by neighboring whiskers, often exhibiting receptive fields spanning several vibrissae beyond the PW (Armstrong-James and Fox 1987; Chapin 1986; Higley and Contreras 2003; Kleinfeld and Delaney 1996; Moore and Nelson 1998; Simons 1978; Zhu and Connors 1999).

Integration of synaptic responses evoked by deflection of multiple whiskers is dependent on the temporal relationship of the stimuli. Previously, we showed that the PW-evoked response was strongly suppressed by a 20-ms prior deflection of a small number of remote whiskers (RWs) far removed from the PW (Higley and Contreras 2003). The mechanism underlying suppression was neither shunting nor hyperpolarizing inhibition but most likely the withdrawal of input, or disfacilitation. Extracellular recordings have demonstrated that the suprathreshold response to PW deflection is also suppressed by prior deflection of an immediately adjacent whisker (AW) at intervals ranging from 10 to 100 ms (Simons 1985; Simons and Carvell 1989). Although the mechanisms are unknown, AW-mediated suppression has been proposed to be based on intracortical lateral inhibition (Goldreich et al. 1999; Kleinfeld and Delaney 1996; Moore et al. 1999; Simons 1985). In addition, other extracellular studies have shown that simultaneous or near-simultaneous deflection of 2 whiskers can result in summation without suppression where the combined spike output is greater than either individual response alone (Ghazanfar and Nicolelis 1997; Mirabella et al. 2001; Shimegi et al. 1999).

The present study was designed to explore whether AW–PW interactions differ phenomenologically and mechanistically from RW-mediated suppression and to elucidate the nature of whisker response interactions at shorter intervals. We found

Address for reprint requests and other correspondence: D. Contreras, Department of Neuroscience, University of Pennsylvania School of Medicine, 215 Stemmler Hall, Philadelphia, PA 19106-6074 (E-mail: diegoc@mail.med.upenn.edu).

The costs of publication of this article were defrayed in part by the payment of page charges. The article must therefore be hereby marked "*advertisement*" in accordance with 18 U.S.C. Section 1734 solely to indicate this fact.

that prior AW deflection at a 20-ms interval strongly suppressed the response to subsequent PW deflection by a mechanism consistent with disfacilitation. At a 3-ms interdeflection interval, suppression was weak or absent. Additionally, using electrical stimulation of the cortex, we found that cortical neurons are capable of integrating responses without suppression at both 3- and 20-ms intervals. These findings suggest that the temporal relationship of sensory-evoked responses is critical in determining the cell's output and that the suppression caused by preceding AW deflection arises from the sensory-induced engagement of cortical and subcortical circuits, resulting in withdrawal of subsequent excitatory drive rather than direct inhibition.

METHODS

Surgery and preparation

Experiments were conducted in accordance with the ethical guidelines of the National Institutes of Health and with the approval of the Institutional Animal Care and Use Committee of the University of Pennsylvania. Adult male Sprague–Dawley rats (400–600 g) were anesthetized with isoflurane (0.5–2.0%). Dexamethasone [10 mg/kg, administered intraperitoneally (ip)], metoprolol (100 mg/kg, ip), and glycopyrrolate (0.025 mg/kg, ip) were administered to reduce brain swelling, blood pressure, and secretions, respectively. Animals were paralyzed with gallamine triethiodide and artificially ventilated. End-tidal CO_2 (3.5–3.7%) and heart rate were continuously monitored. Body temperature was maintained at 37°C by servocontrolled heating blanket and rectal thermometer. The depth of anesthesia was maintained by adjusting the percentage of inspired isoflurane to keep a low heart rate (250–300 beats/min) and constant high-amplitude, low-frequency electroencephalogram as recorded from a bipolar tungsten electrode lowered into the cortex.

For cortical intracellular recordings, the animal was placed in a stereotaxic apparatus and a craniotomy was made to expose the surface of the barrel cortex (1.0–3.0 mm posterior to bregma, 4.0–7.0 mm lateral to the midline). The dura was resected over the recording area, and mineral oil was applied to prevent desiccation. The stability of recordings was improved by drainage of the cisterna magna and filling of the craniotomy with a solution of 4% agar after electrode placement.

Electrophysiological recordings

Intracellular recordings were performed with glass micropipettes pulled on a P-97 Brown–Flaming puller (Sutter Instrument, Novato, CA). Pipettes were filled with 3 M potassium acetate and had DC resistances of 70–90 MΩ. For some recordings, neurobiotin (2.75%) was included in the pipette solution. The recording pipette was lowered into the brain oriented normal to the cortical surface. Vertical depth was read on the scale of the micromanipulator and verified histologically for recovered neurobiotin-filled cells (see Fig. 1). A high-impedance amplifier (band-pass filter of 0–5 kHz) with active bridge circuitry (Cygnus Technology, Delaware Water Gap, PA) was used to record and inject current into the cells. Data were digitized at 10 kHz using a Power 1401 data-acquisition system and Spike2 software (Cambridge Electronic Design, Cambridge, UK) and saved to disk for off-line analysis.

Whisker stimulation

Before recording, whiskers were trimmed to approximately 10 mm. Individual whiskers were mechanically deflected using ceramic piezoelectric bimorph stimulators (custom-made; Piezo Systems, Cambridge, MA) as described previously (Simons 1983; Wilent and Contreras 2004). After obtaining a stable intracellular recording, the distal 2 mm of a whisker was fit snugly into the barrel of a glass capillary attached to the end of the stimulator. Square electrical pulses (200-ms duration) were applied to the stimulator, resulting in a step-and-hold deflection of the whisker of about 750 microns. For all experiments described here, the whiskers were deflected in a dorsal direction. Given the extensive subthreshold receptive fields of barrel cortex neurons (Brecht and Sakmann 2002; Higley and Contreras 2003; Moore and Nelson 1998; Zhu and Connors 1999), 6 whiskers (at a minimum) were tested for each cell to determine the PW, defined as the whisker that evoked the largest depolarizing response from resting membrane potential (Vm). To maintain consistency with previous studies, we also determined the whisker that evoked the most spikes per deflection for those cells that exhibited a suprathreshold response. In all cases, the whisker evoking the largest depolarization also elicited the highest spike counts. Stimuli were delivered at ≤0.5 Hz to prevent steady-state adaptation of whisker-evoked responses (Moore and Nelson 1998). AWs were deflected using a second piezo stimulator. For each cell, the AW was chosen from the 8 surrounding whiskers. For the experiments described here, the AW was deflected alone or preceding the PW by 20 or 3 ms.

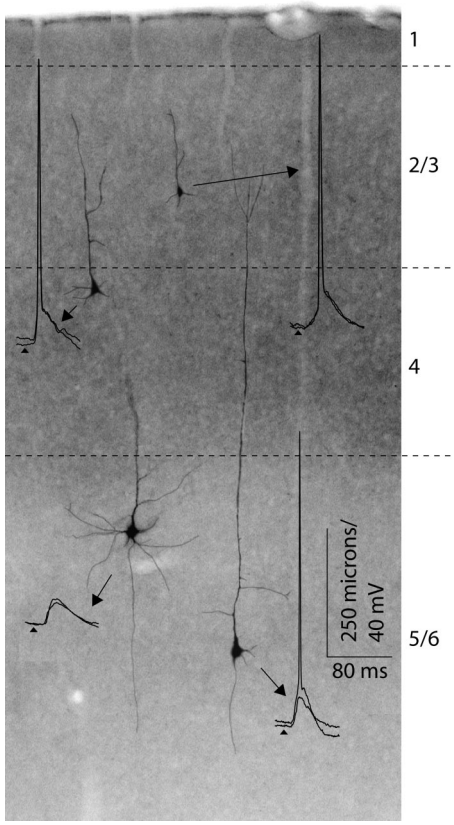

FIG. 1. Examples of barrel cortex neurons recorded in vivo. Neurobiotin-filled examples of a supragranular pyramidal cell recorded at depth of 330 μm, a granular layer pyramid at 534 μm, and 2 infragranular pyramids at 970 and 1205 μm, respectively. Cells were recorded from different experiments and were photographed and superimposed according to their original position on a common Nissl-stained background. Two *superimposed traces* illustrating responses to principal whisker (PW) deflection are shown for each cell (indicated by arrows). Small triangles indicate time of whisker deflection. Three of the cells exhibited suprathreshold responses.

Electrical stimulation

We also examined the integration of responses to cortical electrical stimulation. Each stimulating electrode consisted of 2 insulated tung-

sten wires (75 μm diameter, impedance at 1 kHz was 30–50 kΩ; Frederick Haer, Brunswick, ME) in a bipolar arrangement with 50-μm vertical tip separation. For electrical stimulation experiments, 2 such stimulating electrodes were lowered into the cortex at a depth of about 500–1,000 μm and about 1.0 mm from each other (see Fig. 9). The intracellular recording pipette was placed 500–1,000 μm distant from both stimulating electrodes. Electrical stimulation consisted of 0.1-ms pulses (10–150 μA). The intensity was adjusted for each cell to obtain evoked response amplitudes comparable to those seen with whisker deflection.

Data analysis

All data analysis was done off-line. Routines for spike removal and averaging of sensory responses were written in Igor Pro (Wavemetrics, Lake Oswego, OR). Spikes were removed by detecting the spike threshold at the base of the action potential and extrapolating the Vm values from the start to the end of the spike, followed by smoothing with a 3-point running average. For all cells, baseline Vm was calculated as the mean Vm for the 100 ms preceding the stimulus. Evoked postsynaptic potential (PSP) onset latency was determined by visual inspection of the averaged response and defined as the first time point at which the Vm clearly deviated from baseline at the start of the response. The amplitude of the PSP was measured at the peak depolarization. The rate of rise for each PSP was measured by calculating the slope of the line connecting the points of 10 and 90% peak amplitudes for each response. The apparent input resistance (Rin) of the cell was calculated for the baseline condition as well as for various time points within the stimulus response by evoking a PSP while holding the cell at different Vms using injected DC current (see Fig. 2). Rin was defined as the slope of the best-fit line for a plot of Vm against injected current (*V–I* plot) at each time point. We generally expressed this value relative to the baseline Rin by calculating the fractional Rin ($Rin_{PSP}/Rin_{baseline}$). The apparent reversal potential (Vrev) at selected time points during the synaptic response was calculated as the *y*-value of the intersection of the *V–I* plot made at baseline with the *V–I* plot made at each point. An example of the method is shown in Fig. 7*B*. Because of the low-pass characteristics of the cell membrane, these calculated values likely underestimate the actual synaptic voltage changes occurring at synapses located in the distal dendrites. For those cells that exhibited a suprathreshold response to whisker deflection, we quantified the cell output by calculating the average number of spikes per deflection occurring from 5 to 25 ms poststimulus. All statistical measures were calculated using Prism (GraphPad Software, San Diego, CA).

Histology

At the end of each experiment where neurobiotin was included in the recording pipette, the animal was given a lethal dose of sodium pentobarbital and perfused intracardially with 0.9% saline followed by cold 4% paraformaldehyde in 0.1 M sodium phosphate buffer (PBS). The brain was removed and postfixed overnight in the same fixative. Coronal sections (100 μm thick) were cut on a vibratome, washed 3 times in PBS, and preincubated for 1 h at room temperature in PBS with 10% normal goat serum (Vector Laboratories, Burlingame, CA), 1% albumin from bovine serum (BSA, Sigma, St. Louis, MO), and 0.4% Triton X-100 (Sigma). Sections were then incubated overnight at room temperature in the previous solution containing 0.1% Cy3-conjugated streptavidin (Jackson ImmunoResearch, West Grove, PA). After several rinses with PBS, the tissue was mounted on gelatinized glass slides and coverslipped with Vectashield (Vector Laboratories). Cy3-labeled cells were visualized with an Olympus BX51 microscope (Olympus America, Melville, NY) and a filter cube set for TRITC/DiI/Cy3 (excitation 540 nm, dichroic 565 nm, emission 605 nm; Chroma Technology, Rockingham, VT). Pictures were taken using an Olympus MagnaFire digital camera.

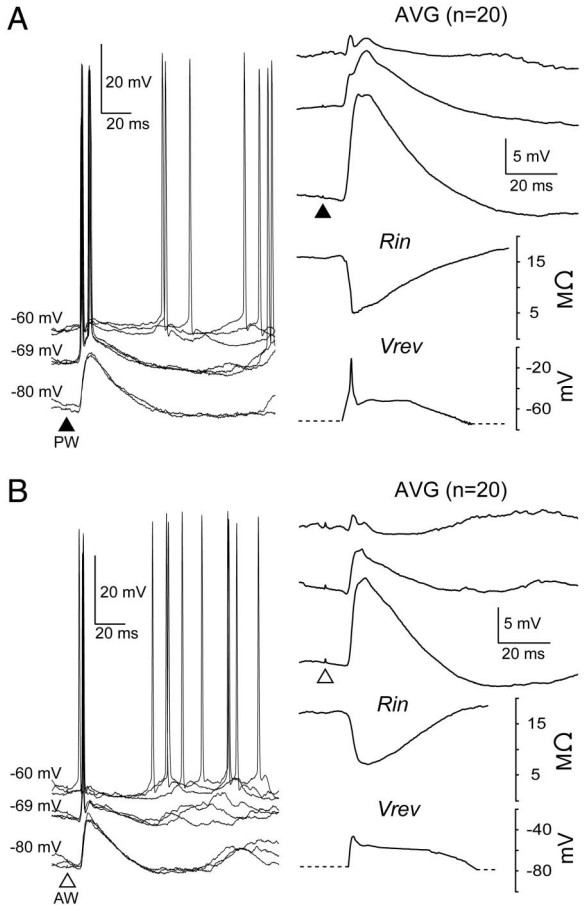

FIG. 2. Representative whisker-evoked responses in a barrel cortex neuron. *A*: a regular-spiking (RS) cell at a depth of 1287 μm responded to step-and-hold deflections of the PW with excitation followed by inhibition. Vm at rest (−69 mV) was displaced to depolarized (−60 mV, 0.40 nA) and hyperpolarized (−80 mV, −0.76 nA) levels by current injection. *Left traces*: 2 individual superimposed responses at each Vm. Filled triangle indicates time of whisker deflection. *Top right traces*: averaged responses (AVG, $n = 20$) at each Vm. Below are plots of the calculated continuous input resistance (*Rin*) and reversal potential (*Vrev*) throughout the synaptic response. *B*: same plots as in *A* for response to adjacent whisker (AW) deflection (open triangle) in the same cell.

RESULTS

We recorded intracellularly from 71 neurons in the barrel cortex of 37 isoflurane-anesthetized rats. Of these cells, 47 met our criteria for analysis: *1*) a stable resting Vm of at least −60 mV throughout the recording; *2*) action potentials overshooting 0 mV; and *3*) PW-evoked response onset latencies of <10 ms to minimize the inclusion of cells located above, below, or within the barrel septa (Brecht and Sakmann 2002; Brecht et al. 2003). The resting Vm for all cells was −69 ± 7 mV (mean ± SD), and the Rin at rest was 23.7 ± 8.3 MΩ. The spontaneous firing rate for all cells was 2.2 ± 1.5 Hz. Several cells ($n = 11$) were filled with neurobiotin during recording and recovered histologically. For these cells, the actual cortical depth did not vary from the depth read on the micromanipulator by more than 25 μm. Figure 1 illustrates 4 recovered pyramidal cells spanning cortical layers 3–5. These cells were recorded in different experiments, photographed, and arranged on a common Nissl-stained background according to their original cortical location. For each cell, 2 *superimposed traces*

illustrating responses to PW deflection are shown (indicated by arrows). Small triangles indicate the time of whisker deflection.

Synaptic responses to whisker deflection

To study the integration of synaptic responses to sensory stimulation within individual barrel cortex neurons, we deflected the PW and one AW for 37 cells. Whisker stimuli consisted of a step-and-hold deflection in a fixed dorsal direction from the resting position. For each cell, the PW was defined as the whisker whose deflection caused the largest depolarizing response from baseline at rest. For cells in which a suprathreshold response could be elicited, we also determined the whisker that evoked the greatest number of spikes. In all cases, deflection of the PW also evoked the most spikes per deflection. For each cell, the AW was chosen from the 8 whiskers surrounding the PW. In a small number of cells (n = 5), we tested multiple AWs and observed some variability in response magnitude, consistent with previous findings (Simons and Carvell 1989). For these cases, only the AW evoking the largest amplitude response was included for analysis. Post hoc analysis of the entire population revealed no significant differences for any measure between different AW positions. Therefore data from all experiments were combined as simply "AW."

The whisker-evoked postsynaptic potential (PSP) at rest generally consisted of an early depolarization often followed by a delayed hyperpolarization. To characterize the whisker-evoked PSP, we deflected the PW while holding the cell at different Vm levels using current injection through the micropipette (Fig. 2). Previous studies have demonstrated that measuring an evoked PSP at different Vm levels allows a qualitative description of the different synaptic components and calculation of the apparent Vrev and change in Rin (Anderson et al. 2000; Borg-Graham et al. 1998; Coombs et al. 1955a; Hirsch et al. 1998; Lang and Pare 1997, 1998; Monier et al. 2003; Moore and Nelson 1998). Figure 2*A* shows responses to PW deflection in a regular-spiking (RS) cell (1,287 μm depth). On the left, 2 *individual traces* are superimposed for each of 3 Vm levels: rest (−69 mV, 0 nA), hyperpolarized (−80 mV, −0.76 nA), and depolarized (−60 mV, +0.40 nA). PW deflection elicited suprathreshold PSPs at both resting and depolarized levels. The averaged PSPs (n = 20 trials) are shown in the *top right* and labeled AVG (spikes removed, see METHODS). The PSP to PW deflection at resting Vm consisted of an initial depolarization with a 7.5-ms onset latency that peaked at 17.1 ms; it had an amplitude of 7.8 mV and was followed by a longer lasting hyperpolarization.

We calculated the apparent Rin as a continuous function of time by plotting the value of averaged Vm against injected current at each time point before and during the averaged PSP (Fig. 2, *Rin*, see METHODS). For this cell, the baseline steady-state Rin was 15.5 MΩ and decreased to an apparent minimal value of 5.0 MΩ near the peak of the response (a fractional Rin of 0.32). We also calculated the apparent Vrev as a function of time (Fig. 2, *Vrev*; see METHODS). The PW-evoked PSP consisted of an early component that reversed at −9 mV, most likely dominated by fast excitatory glutamatergic input, followed by a longer component that reversed near −55 mV, probably dominated by chloride-mediated γ-aminobutyric acid-A ($GABA_A$) inhibition.

For the same cell, we characterized the response to deflection of one AW (Fig. 2*B*). The AW-evoked PSP occurred at a slightly longer onset latency (8.3 ms) and had a smaller amplitude at rest (5.5 mV) as compared with the PW-evoked PSP. AW deflection caused a reduction in apparent Rin from a baseline value of 17.7–7.0 MΩ near the peak of the depolarization (a fractional Rin of 0.40). The apparent Vrev of the AW-evoked PSP also showed an early fast excitation, although it reached a peak less depolarized than for the PW deflection (−42 mV), suggesting that excitation and inhibition may overlap earlier during the AW response.

The quantification of whisker responses for the population (n = 37) is shown in Table 1. For each parameter, the mean ± SD value is given (see METHODS). Statistical significance for the paired comparison of PW and AW data are shown at the *right*. In summary, the typical response pattern to whisker deflection was an initial depolarization that frequently evoked action potentials and was accompanied by a large decrease in the Rin of the cell. Furthermore, response to PW deflection generally occurred with a shorter onset latency, faster rise time, and larger peak amplitude compared with AW deflection.

Integration of sensory responses

Previous intracellular work has demonstrated that deflection of remote whiskers 20 ms before the PW strongly suppresses the PW response (Higley and Contreras 2003). However, extracellular studies have shown that deflection of AWs at shorter intervals (0–5 ms) may lead to response summation without suppression (Ghazanfar and Nicolelis 1997; Mirabella et al. 2001; Shimegi et al. 1999). To further study the spatial and temporal dependency of whisker-evoked response integration, we deflected the AW before the PW at intervals of 20 and 3 ms. A representative example of an RS cell (1,501 μm depth) is shown in Fig. 3*A*. Peristimulus time histograms on the *left* illustrate the spike output of the cell-to-whisker deflection. PW deflection evoked 0.6 spikes/deflection, whereas AW deflection evoked 0.5 spikes/deflection. At an interdeflection interval of 20 ms, the PW-evoked response was reduced to 0.2 spikes/deflection. In contrast, at the 3-ms interval, the spike output was increased to 0.9 spikes/deflection. We quantified the effect of preceding AW deflection by calculating a response ratio as the spikes per deflection evoked by the PW when preceded by the AW divided by the spikes per deflection to the PW alone. Thus a response ratio <1 indicates suppression. This measure is similar to the method of Simons (1985). For the cell in Fig. 3*A*, the spike response ratio at the 20-ms interval was 0.33, whereas at the 3-ms interval the spike response ratio was 1.50.

TABLE 1. *Summary and comparison of response parameters to PW and AW deflection*

	PW	AW	Paired t-Test
Latency to onset (ms)	7.6 ± 2.0	8.5 ± 2.3	$P < 0.01$
Latency to peak (ms)	15.1 ± 4.0	16.5 ± 4.2	$P < 0.01$
Peak amplitude (mV)	8.3 ± 3.7	6.5 ± 4.3	$P < 0.001$
Spikes per deflection	0.9 ± 0.7	0.6 ± 0.6	$P < 0.05$
Peak fractional Rin	0.60 ± 0.22	0.66 ± 0.25	n.s.
dV/dt (mV/ms)	2.2 ± 1.3	1.6 ± 1.2	$P < 0.01$

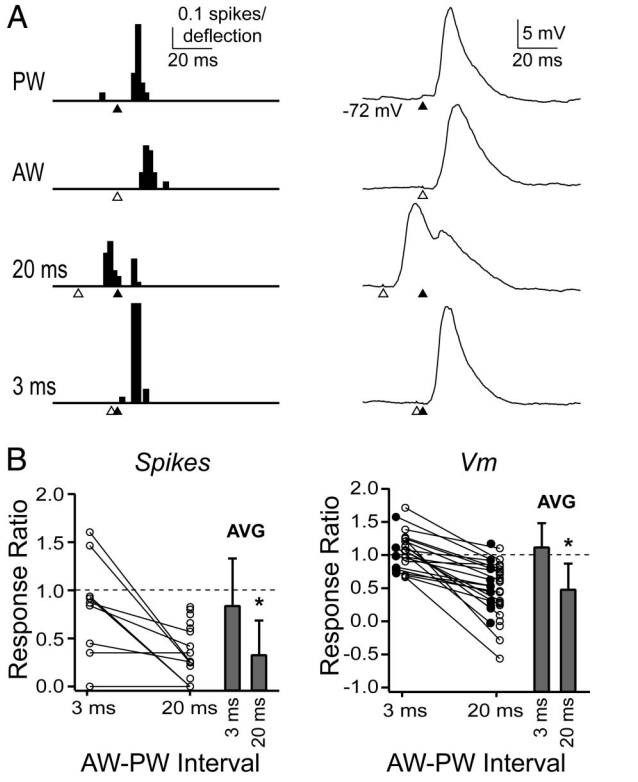

FIG. 3. Interaction of PW and AW responses at different interdeflection intervals. *A*: example of an RS cell at 1501 μm depth. *Left histograms*: cumulative spike output (in spikes per deflection, bin size = 5 ms). *Right traces*: averaged synaptic responses (n = 20–30 deflections) at rest (−72 mV). Responses to PW deflection alone, AW deflection alone, and PW preceded by AW at 20 and 3 ms are shown. Open (AW) and filled (PW) triangles indicate time of whisker deflection. Spike output and peak depolarization to deflection of the PW alone were reduced at the 20-ms interval and increased at the 3-ms interval. *B*: summary of changes in spike and Vm responses to PW deflection for the whole population. Response ratio was calculated as the magnitude of the AW–PW response divided by the PW response alone. Circles represent the value of this ratio for spike output on the *left* (*Spikes*) and peak level of depolarization on the *right* (*Vm*). For Vm data, cells with suprathreshold responses to PW deflection (open circles) are horizontally offset from cells with exclusively subthreshold responses (filled circles). Lines connect values from the same cell over the 2 AW–PW intervals, 3 and 20 ms. Bars indicate the mean response ratios ± SD for each interval. Average response ratio was significantly <1 at the 20-ms interval for both spikes ($P < 0.01$) and Vm ($P < 0.01$). Values at the 3-ms interval did not differ significantly from 1 for either spikes or Vm.

We also measured the corresponding whisker-evoked synaptic responses (*right traces* are averaged responses to 20–30 deflections). For this cell, PW deflection caused a 15.8 mV PSP from a baseline Vm of −72 mV (peak Vm = −56.2 mV), whereas AW deflection caused a 13.8 mV PSP (peak Vm = −58.2 mV). At the 20-ms interval, the PW-evoked PSP, riding on the decaying depolarization of the AW-evoked response, reached a peak depolarization of 10.4 mV from baseline (peak Vm = −61.6 mV), whereas at the 3-ms interval, the combined response reached a peak depolarization of 16.6 mV (peak Vm = −55.4 mV). Therefore the increase or decrease in spike output in response to paired whisker deflection can be explained by the corresponding increase or decrease in the peak level of depolarization reached by the underlying PSP. To quantify this change in depolarization, we calculated a Vm response ratio as the peak depolarization from baseline caused by PW deflection when preceded by the AW divided by the peak depolarization from baseline caused by PW deflection alone. Thus a Vm response ratio <1 indicates that preceding AW deflection caused the PW-evoked response to reach a peak Vm less depolarized than PW deflection alone. In contrast with spike data, the Vm can assume values below baseline, leading to a negative Vm response ratio in some cases. For the cell in Fig. 3*A*, the Vm response ratio was 0.66 (10.4 mV/15.8 mV) at the 20-ms interval and 1.05 (16.6 mV/15.8 mV) at the 3-ms interval.

We quantified the effect of a preceding AW deflection on the spike output for the population of cells (Fig. 3*B*, *Spikes*). When the AW preceded the PW by 20 ms, there was a suppression of the PW-evoked spikes for 20/20 cells. The average response ratio was 0.30 ± 0.30 and was significantly <1 (Student's t-test, $P < 0.001$). These response ratio values are comparable to previous findings from extracellular studies of cross-whisker interactions (Mirabella et al. 2001; Shimegi et al. 1999; Simons 1985; Simons and Carvell 1989), indicating that our intracellular recordings did not compromise cell integrity and spike output. When AW deflection preceded PW deflection by 3 ms, the spike output was suppressed for 7/9 cells, although the average response ratio (0.83 ± 0.51) was not significantly different from 1.

We also quantified the Vm response ratios for the population (Fig. 3*B*, *Vm*). Values for cells exhibiting suprathreshold responses (open circles) are offset horizontally from cells exhibiting exclusively subthreshold responses (filled circles). However, no significant difference was found between these 2 groups, and the data were pooled for further analysis. At the 20-ms interval, the Vm response ratio was <1 for 35/37 cells (average Vm response ratio = 0.49 ± 0.38; $P < 0.001$). However, when the interval was reduced to 3 ms, the effect was weak reduction in peak depolarization (Vm response ratio never <0.6) for 8/21 cells, although the average response ratio (1.08 ± 0.27) was not significantly different from 1. In summary, deflection of an AW 20 ms before PW deflection reliably leads to reduction of both the PW-evoked spike output and the underlying peak level of depolarization. In contrast, when the interdeflection interval is 3 ms, the average result is an absence of suppression.

Prior whisker deflection divisively reduces PW-evoked PSP amplitude

Suppression of spike output occurs subsequent to a reduction in the peak level of depolarization evoked by the PW. This reduction can be explained either by *1*) hyperpolarizing the baseline Vm or *2*) decreasing the amplitude of the PSP. These 2 processes are equivalent to the algebraic operations of addition and multiplication, respectively, and correspond to well-characterized cellular processes (Coombs et al. 1955b; Holt and Koch 1997; Llinas et al. 1974). Examples are illustrated in the recordings shown in Fig. 4*A*. Each set of *superimposed traces* includes the averaged PSP to the PW deflection alone (light gray), AW deflection alone (medium gray), and PW preceded 20 ms by AW (dark gray). To estimate the contribution of each algebraic operation, we made 3 measurements for each cell: *a*, the peak amplitude of the PW-evoked PSP as measured from baseline; *b*, the Vm offset caused by the preceding AW-evoked PSP; and *c*, the amplitude of the PSP

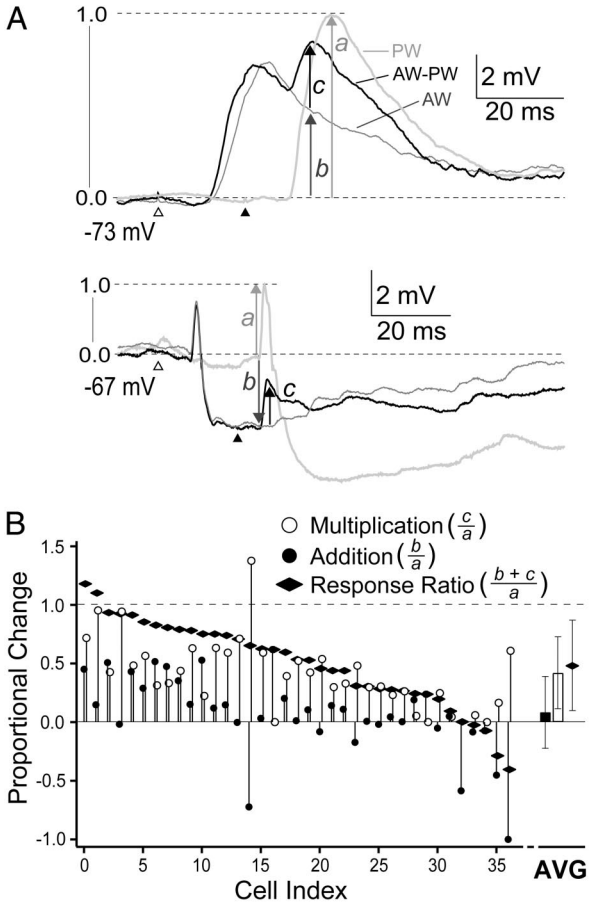

FIG. 4. Contribution of addition and multiplication components to Vm response ratio values at the 20-ms interdeflection interval. *A*: 2 examples of the responses to deflection of the PW (light gray), AW (medium gray), and PW preceded 20 ms by AW (dark gray). Triangles indicate times of whisker deflection. For each case, measured values were: *a*, amplitude of postsynaptic potential (PSP) evoked by PW alone; *b*, shift in Vm caused by the AW alone; and *c*, amplitude of the PW-evoked PSP when preceded by the AW, estimated from the previously measured *b*. In the *top example*, the PW response rode on an AW-evoked depolarization ($b > 0$), whereas in the *bottom example* the PW response rode on a hyperpolarization ($b < 0$). In both cases, the amplitude of the PW evoked response is reduced by previous AW deflection (i.e., $c < a$). *B*: response ratio (diamonds) was calculated as the peak depolarization from baseline of the PW-evoked response when preceded by the AW, divided by the peak depolarization from baseline of the PW-evoked response alone [(b + c)/(*a*)]. Values <1 indicate suppression. Proportional change contributed by the addition component (filled circles) was calculated as the shift in baseline as a fraction of the PW-evoked response amplitude (*b*/*a*). Values of addition <0 indicate a subtractive effect (baseline shifted down), and values >0 indicate an additive effect (baseline shifted up). Proportional change contributed by the multiplication component (open circles) was calculated as the fractional change in the PSP amplitude evoked by the PW (*c*/*a*). Values of multiplication <1 indicate a divisive effect (PSP amplitude decreased), and values >1 indicate a multiplicative effect (PSP amplitude increased). Response ratio is equal to the sum of the addition and multiplication components. Points are in order of decreasing response ratio. Average values ± SD are indicated to the *right* (AVG).

evoked by deflection of the PW when preceded by the AW, measured from *b*.

To compare across cells, these values were normalized by the amplitude of the PSP evoked by the PW alone (*a*). We derived an addition component, expressed as the ratio *b*/*a*, which represents the amount of hyperpolarizing (subtractive) or depolarizing (additive) offset acting on the baseline of the PW-evoked PSP when preceded by the AW. We also derived a multiplication component, expressed as *c*/*a*, which represents the fractional change in PW-evoked PSP amplitude. The response ratio, as shown in Fig. 3, is the sum of these measures, or $(b + c)/a$, and is equivalent to the ratio of the peak level of depolarization from baseline of the PW-evoked PSP when preceded by AW deflection to the peak level of depolarization from baseline of the PW-evoked PSP alone.

For the example in the *top traces* of Fig. 4*A* (RS cell, 326 μm depth), the AW evoked a long-lasting depolarization such that (*b*/*a*) was positive, or additive. In the lower example (RS cell, 1,037 μm depth), the AW evoked a fast large hyperpolarization. For this case, the value of (*b*/*a*) was negative, indicating a subtractive effect. However, the amplitude of the PW-evoked PSP was reduced in both examples [i.e., (*c*/*a*) <1], indicating a concurrent divisive effect.

We calculated the contribution of addition and multiplication components to the response ratio at the 20-ms interval for each cell (Fig. 4*B*). The Vm response ratio data from Fig. 3*B* are represented here as diamonds, and the data points are shown in order of decreasing response ratio. The multiplication component (open circles) was <1 (a divisive effect) in all but one cell (average multiplication = 0.42 ± 0.29). The addition component (filled circles) was depolarizing in the majority of cells ($n = 22/37$), yielding an average addition component of 0.07 ± 0.34. Across all cells, the response ratio values were weakly correlated with the multiplication values (Pearson's correlation; $r^2 = 0.27$; $P < 0.001$) and more strongly correlated with the addition values ($r^2 = 0.47$; $P < 0.001$). These results demonstrate that a strong divisive amplitude reduction occurs in almost all cells. However, this divisive operation can act either on an additive or subtractive background that may reduce or enhance the change in peak depolarization depending on the exact nature of the AW-evoked PSP, which varies between cells.

Several mechanisms may explain the divisive amplitude reduction caused by preceding AW deflection. AW deflection most often evoked a depolarization that would decrease the synaptic driving force on subsequent PW-evoked input (Bush and Sejnowski 1994). To address this possibility, for those cells where whisker responses were recorded at multiple Vm levels, we plotted the amplitude of the PW-evoked synaptic response against the baseline Vm. An example of this method is shown in Fig. 5*A*. The values of the PW-evoked PSP amplitude at different Vm levels are indicated by filled squares and were well fit by a linear regression. The PSP amplitude from resting Vm was 11.2 mV (denoted *a*, following Fig. 4*A*). At the 20-ms interval, the preceding AW deflection resulted in a depolarization of 7.3 mV (denoted *b*). The regression line was used to extrapolate the expected PW-evoked amplitude at the shifted baseline Vm of −69.7 mV. The expected value was 9.4 mV (denoted *a*′), although the actual PW-evoked PSP amplitude when preceded by AW deflection was only 5.6 mV (denoted *c*).

For the population, we plotted the obtained values of PW-evoked PSP amplitude when preceded by AW deflection at the 20-ms interval against the extrapolated expected amplitudes (Fig. 5*B*). The data showed a significant but weak correlation ($r^2 = 0.27$, solid line; $P < 0.01$), indicating that driving force does play a role in reducing the PSP amplitude. However, all of the data points fell below unity (dashed line), indicating that in all cases, the observed amplitude was reduced more than

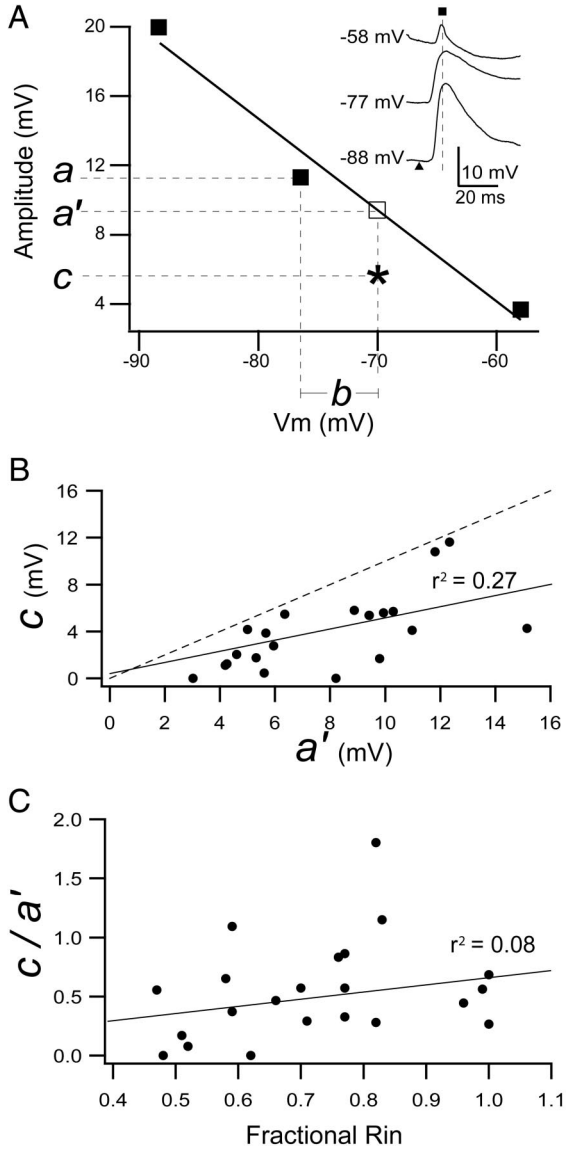

FIG. 5. Contribution of driving force and shunting to the reduction in response amplitude. *A*: plot of PW-evoked PSP amplitude vs. baseline Vm for 3 different Vm levels set using DC current injection through the recording pipette (filled squares; see *inset traces*). PSP amplitude at resting Vm is indicated by *a*. Linear regression of the data points was used to predict the PW-evoked PSP amplitude (open square, *a′*) after the depolarizing Vm offset caused by preceding AW-evoked response (*b*). Actual recorded PW-evoked PSP amplitude (*c*) is indicated by the asterisk. *B*: obtained value of PW-evoked PSP amplitude after AW deflection (*c*) at the 20-ms interval was plotted against the predicted PW-evoked PSP amplitude (*a′*). Data points were weakly correlated ($r^2 = 0.27$, solid line; $P < 0.01$), but all values fell below unity (dashed line), indicating that the obtained amplitude was smaller than predicted for all cells. *C*: plot of (*c*/*a′*) vs. the fractional Rin of the AW-evoked response at the time corresponding to the PW-evoked PSP onset. Change in PSP amplitude did not correlate with the change in Rin ($r^2 = 0.08$, solid line; not significant).

could be accounted for by the decrease in driving force. This finding suggests that some additional mechanism contributes to the divisive amplitude reduction.

A second cellular mechanism by which AW deflection may divisively reduce the PW-evoked PSP amplitude is by reducing the Rin of the cell (shunting inhibition). If synaptic shunting plays a role, the decrease in amplitude should correlate with the drop in Rin caused by the preceding AW deflection. To discount the effects of driving force on the PSP, we calculated the ratio of the observed PSP amplitude divided by the expected value, which is corrected for the change in Vm. We plotted the resulting value (denoted *c*/*a′*) against the fractional decrease in Rin caused by the AW-evoked PSP at the time corresponding to the onset of the PW-evoked response (see METHODS). The axes cover a range from 0 (at which there is a total elimination of the PW-evoked PSP and a total disappearance of measurable Rin) to 1 (at which the PW-evoked amplitude is unchanged and there is no decrease in Rin). If the amplitude reduction were exclusively attributable to a decrease in Rin, one would expect a linear (ohmic) relationship between the plotted variables. However, the data did not reveal a correlation ($r^2 = 0.08$, solid line; not significant), suggesting that the divisive amplitude reduction is independent of changes in Rin and that other mechanisms contribute to the effect.

As shown in Fig. 3*B*, the average Vm response ratio for the 3-ms interval did not differ significantly from 1, contrasting with the 20-ms interval data. To understand these disparate findings, we also calculated the relative contributions of multiplication and addition components to integration of responses at the shorter interval (Fig. 6*A*). Vm response ratio data from Fig. 3*B* are shown as diamonds for reference, and the points are in order of decreasing value. Similar to the 20-ms interval, all cells ($n = 21$) exhibited a multiplication component <1 (open circles; average multiplication $= 0.35 \pm 0.23$). In contrast to the 20-ms interval data, all cells exhibited an addition component >0 (filled circles; average addition $= 0.73 \pm 0.30$). Thus the difference in response ratios between the 2 intervals is explained by a similar divisive reduction in PSP amplitude combined with a much larger AW-evoked depolarization at 3 ms.

As with the 20-ms interval data, we attempted to characterize the effect of altered driving force on the PW-evoked response. In Fig. 6*B*, we plotted the observed PW-evoked PSP amplitude after AW deflection at the 3-ms interval against the extrapolated expected value (see Fig. 5). As with the 20-ms interval, the data showed a significant but weak correlation ($r^2 = 0.30$, solid line; $P < 0.05$). However, the majority of points fell below unity (dashed line), indicating that the PSP amplitude was reduced more than expected by the decreased driving force. We then plotted the ratio of the observed amplitude to expected amplitude (*c*/*a′*) against the fractional change in Rin caused by the AW-evoked PSP at the time corresponding to the onset of the PW-evoked response (Fig. 6*C*). The data revealed no correlation ($r^2 = 0.04$, solid line; not significant), suggesting that the change in Rin does not play a dominant role in the integration of responses at this interval and that other mechanisms determine the divisive reduction in amplitude.

AW-mediated disfacilitation of PW-evoked response

At the 20-ms interval, in addition to a reduction of the PW-evoked PSP amplitude, we also observed a consistent decrease in its rate of rise. In Fig. 7*A*, the averaged PSPs of an RS cell (381 μm depth) to PW deflection alone (light gray) and PW preceded 20 ms by AW deflection (dark gray) are superimposed. This cell demonstrated a strong reduction of the PW-evoked PSP amplitude. Furthermore, the 10–90% rate of

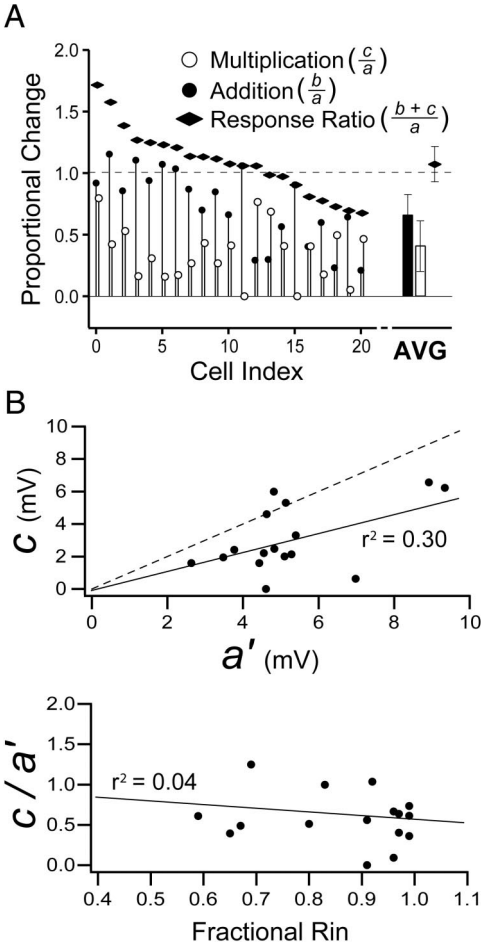

FIG. 6. Contribution of addition and multiplication components to the response ratio values at the 3-ms interdeflection interval. *A*: quantification of addition (filled circles), multiplication (open circles), and response ratio (diamonds) as in Fig. 4. Points are in order of decreasing response ratio. Average values ± SD are indicated to the *right* (AVG). *B*: obtained value of PW-evoked PSP amplitude after AW deflection (c) at the 3-ms interval was plotted against the predicted PW-evoked PSP amplitude (a'). Data points were weakly correlated ($r^2 = 0.30$, solid line; $P < 0.05$), but most values fell below unity (dashed line), indicating that the obtained amplitude was smaller than that predicted for all cells. *C*: plot of (c/a') vs. the fractional Rin of the AW-evoked response at the time corresponding to the PW-evoked PSP onset. Change in PSP amplitude did not correlate with the change in Rin ($r^2 = 0.04$, solid line; not significant).

rise of the PW-evoked PSP (dashed lines) was reduced from 2.9 to 0.6 mV/ms by the preceding AW deflection. This reduction in slope is not consistent with synaptic shunting, because an increased conductance would shorten the cell's time constant and lead to an increased slope. Instead, the decreased slope suggests a reduction in input (disfacilitation), another mechanism by which PSP amplitude can be divisively reduced (Llinas and Terzuolo 1964).

Because the PSPs typically fused at the 3-ms interval and no distinct rising phase of the PW-mediated response was detectable, we were able to measure the PSP slope only for the 20-ms interval across the population. We plotted the ratio of the observed PSP amplitude to the expected value (c/a') from Fig. 5*C* against the fractional decrease in dV/dt (i.e., the 10–90% slope of the AW–PW PSP divided by the slope of the PSP to the PW alone) (Fig. 7*B*). Both axes run from 0 (elimination of the PW-evoked PSP and no measurable slope) to 1 (no change in the amplitude or slope of the PSP). First, these data reveal that all cells exhibited a fractional dV/dt value <1, indicating a consistent reduction in the slope of the PW-evoked PSP when preceded by the AW. Second, there is a significant correlation ($r^2 = 0.32$, solid line; $P < 0.01$) between the 2 parameters, suggesting that the mechanism underlying the decrease in dV/dt is also responsible in part for the divisive reduction in the amplitude of the PW-evoked PSP.

Further evidence supporting a withdrawal of input and arguing against shunting inhibition as the principal mechanism underlying the reduction in PSP amplitude was found in 4 cells that exhibited only inhibition in response to whisker deflection and were not included in the previous analyses. This phenomenon was previously observed using extracellular recordings (Sachdev et al. 2000). In these cases, deflection of multiple whiskers revealed no occurrence of whisker-evoked excitation. The PW was defined as the whisker evoking the largest PSP from rest that also occurred with the shortest latency. One example is shown in the RS cell (594 μm depth) in Fig. 8*A*, where the averaged PSPs to PW deflection alone (light gray) and PW deflection preceded 20 ms by AW deflection (dark gray) are superimposed. DC current injection was used to hold the cell at 3 different values of Vm during whisker deflection: resting Vm (−74 mV), a depolarized level (−58 mV, 0.81 nA), and a hyperpolarized level (−87 mV, −0.46 nA). The different Vm levels were used to calculate the apparent Rin and Vrev (Fig. 8*B*; also see METHODS) of the PW-evoked PSP at the times indicated by the dotted lines. The traces reveal that the peak of the PSP to the PW deflection reversed polarity between −65

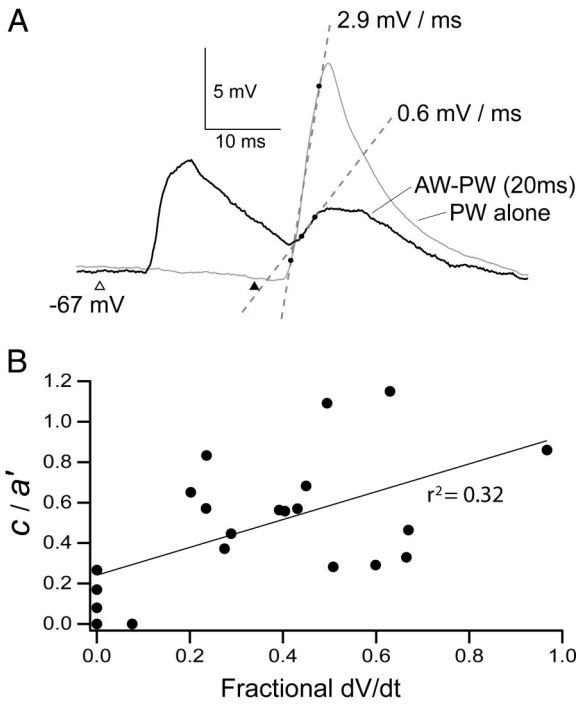

FIG. 7. Slope of the PW-evoked response is reduced by preceding AW deflection. *A*: example of an RS cell at 381 μm depth. *Traces*: average response to PW deflection alone (light gray) and response to PW preceded 20 ms by AW deflection (dark gray). Value of dV/dt of the rising phase of the PSP was calculated as the slope of the line connecting 10 and 90% of the peak amplitude (dashed lines). Preceding AW deflection reduced the dV/dt of the PW response from 2.9 to 0.6 mV/ms. *B*: plot of the (c/a') values from Fig. 5*C* vs. the fractional dV/dt (ratio of the dV/dt of the combined AW–PW response to the dV/dt of the PW-evoked response alone). Data showed a significant correlation ($r^2 = 0.32$, solid line; $P < 0.01$).

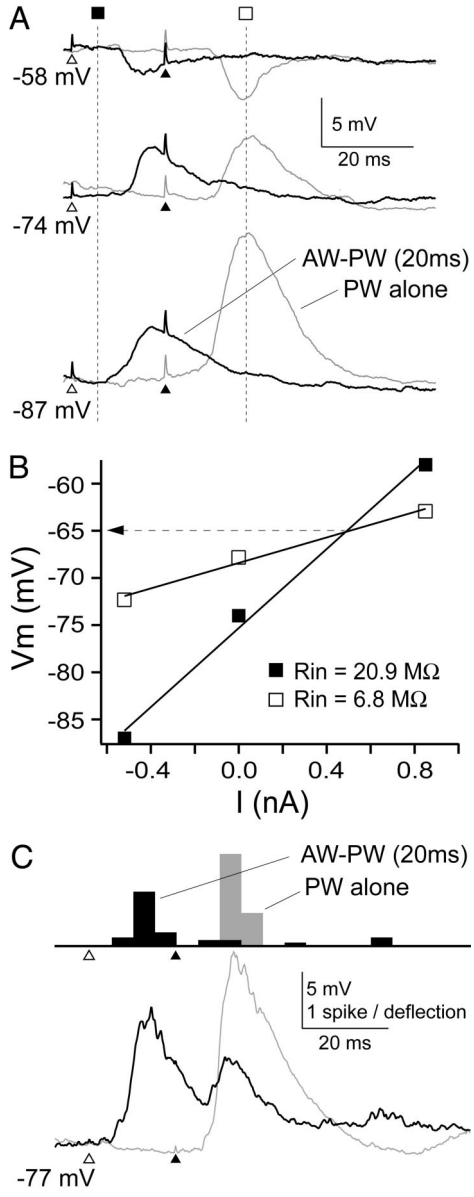

FIG. 8. Prior AW deflection suppresses intracortical inhibition. *A*: example of an RS cell at 594 μm depth. *Top traces*: average response to PW deflection alone (light gray) and response to PW preceded 20 ms by AW deflection (dark gray). Recordings were made at 3 different Vm levels by intracellular DC current injection: rest (−74 mV), depolarized (−58 mV, 0.81 nA), and hyperpolarized (−87 mV, −0.46 nA). *Depolarized traces* show that responses to both PW and AW deflection were hyperpolarizing from −58 mV, indicating responses consisted entirely of inhibition. Preceding AW deflection completely eliminated the PW-evoked IPSP. Vertical dotted lines indicate time of baseline and peak Vm measurement. *B*: *V–I* plot of the PW-evoked response from *A*. Measurements were made at baseline (filled squares) and at the peak of the depolarization from resting Vm (open squares). Lines are the best linear fit to each set of points, and Rin (values indicated) is the slope of the line. Intersection of the 2 lines indicates the apparent reversal potential of the response (dashed line). *C*: example of a fast-spiking cell (presumed interneuron) at 850 μm depth. *Bottom traces*: average responses to PW deflection alone (light gray) and PW deflection preceded 20 ms by AW deflection (dark gray). *Top histograms* indicate the spike output of the cell accumulated over 20 deflections (bin size = 5 ms). Preceding AW deflection strongly reduced the spike response and peak level of depolarization caused by PW deflection.

and −70 mV, suggesting that it was mediated predominantly by a $GABA_A$ chloride conductance. The AW-evoked PSP exhibited similar behavior. Because the 2 PSPs appear to have the same measured Vrev, their underlying conductances should add linearly to bring the Vm closer to that potential. Instead, the response to the PW was virtually absent, indicating that the underlying conductance was not activated and therefore shunting was not responsible for its suppression.

Additional evidence that increased cortical inhibition is not responsible for suppression comes from recordings of fast-spiking cells that are presumed to be inhibitory interneurons ($n = 3$). These cells exhibited high-frequency (>200 Hz) trains of nonadapting, short-duration (<0.7 ms) spikes with pronounced afterhyperpolarizations (Connors and Gutnick 1990; Contreras 2004; Kawaguchi and Kubota 1993). One example of this type of cell is shown in Fig. 8*C*. These cells exhibited a similar suppression of the PW-evoked spike response and reduction in peak depolarization caused by preceding AW deflection as in other cell types.

In an attempt to dissect the synaptic components of the PW-evoked PSP that are altered by the preceding AW deflection, we repeated the paired deflections while holding the cell at different Vm levels. Figure 9 shows an example of an RS cell (330 μm depth) recorded at resting Vm (−76 mV, 0 nA), a depolarized level (−54 mV, 0.64 nA), and a hyperpolarized level (−92 mV, −0.55 nA). At each level, the *averaged traces*

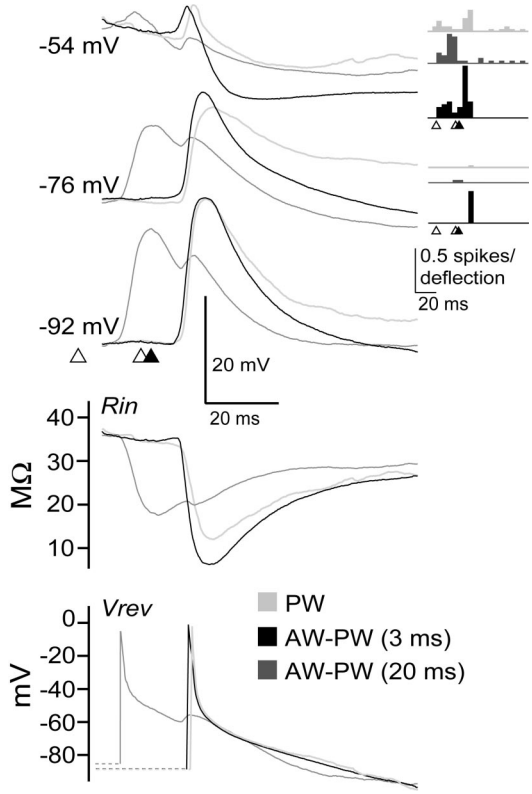

FIG. 9. Preceding AW deflection alters specific components of the PW-evoked synaptic response. *Top traces*: averaged responses to PW deflection alone (light gray), PW preceded by AW at 20 ms (medium gray), and PW preceded by AW at 3 ms (dark gray), each measured at 3 Vm levels: rest (−76 mV), depolarized (−54 mV, 0.64 nA), and hyperpolarized (−92 mV, −0.55 nA) in an RS cell (330 μm depth). Histograms of corresponding spike responses for rest and depolarized Vms are shown in the *inset at right*. PW-evoked spike responses and peak levels of depolarization were reduced at the 20-ms interval but not at the 3-ms interval. *Bottom traces*: calculated plots of continuous input resistance (*Rin*) and reversal potential (*Vrev*) for the 3 stimulus conditions. PW-evoked drop in Rin and early excitatory Vrev peak were suppressed at the 20-ms interval. At the 3-ms interval, the drop in Rin was increased and the early Vrev peak was unaffected.

of the synaptic response to the PW deflection alone (light gray), AW preceding PW by 20 ms (medium gray), and AW preceding PW by 3 ms (dark gray) are shown. Whisker responses were suprathreshold at resting and depolarized Vm levels, and the corresponding spike histograms are shown to the *right*. The traces clearly reveal a strong reduction of the PW-evoked response (both the PSP amplitude and the spikes) at the 20-ms interval. However, at the 3-ms interval, no suppression occurred because the combined response yielded more spikes than the PW alone. Plots of the continuous Rin and Vrev of the PSPs are shown below on separate axes. The Rin plot clearly reveals a large increase in conductance during the response to the PW deflection. At the 20-ms interval, this conductance increase was markedly attenuated, whereas at the 3-ms interval it was increased. The plot of Vrev reveals that the PW-evoked PSP consisted of an early excitation that reversed at −5 mV, consistent with a glutamatergic input, followed by a longer component that reversed between −60 and −80 mV, consistent with GABAergic inhibition. At the 20-ms interval, the early excitation was strongly reduced, although not eliminated, suggesting that the effect of preceding AW deflection was a decrease in the excitatory drive to the cell. At the 3-ms interval, there is little change in the Vrev plot. In summary, these data indicate that at the 20-ms interval, reduction of the PW-evoked response involves a decrease in both excitatory and inhibitory input, as evidenced by the loss of the early peak in Vrev and the reduced drop in Rin. In contrast, at the 3-ms interval, interaction of the AW- and PW-evoked responses involves summation of both excitation and inhibition as shown by the increase in both the spike response and the drop in Rin.

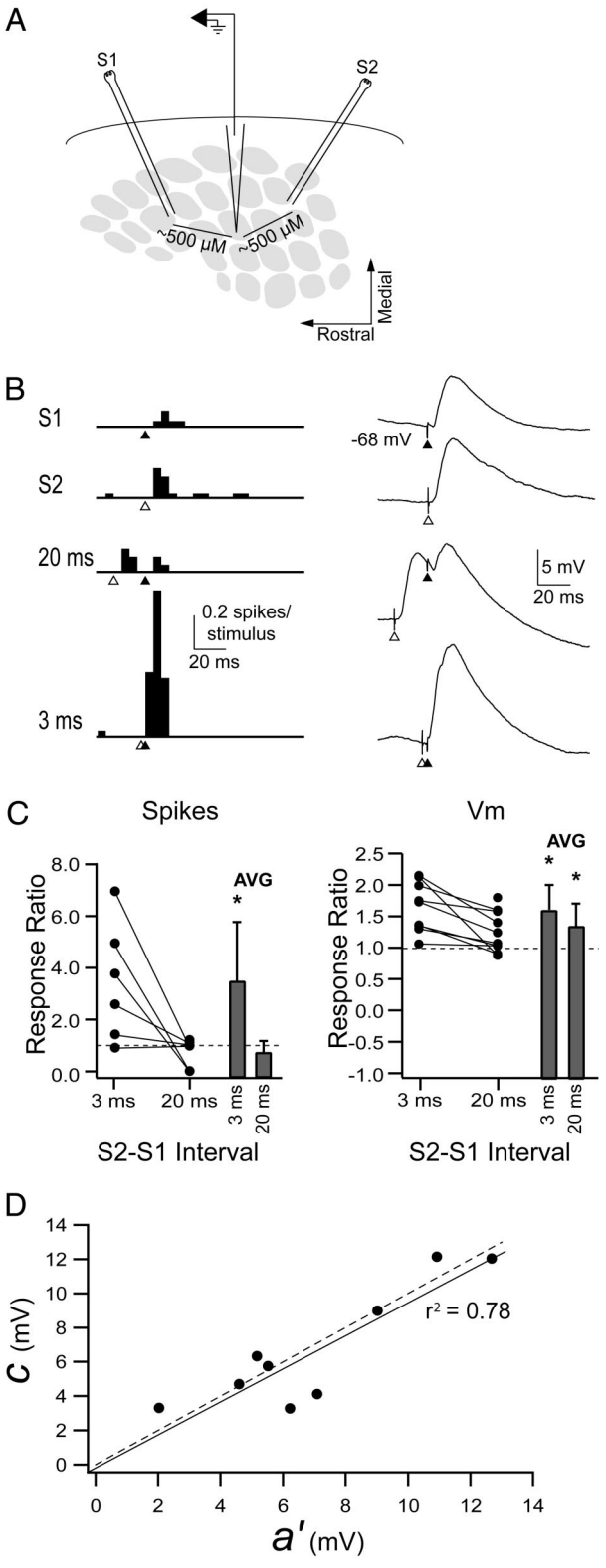

Integration of electrically evoked responses

Synaptic inputs have the ability to engage active dendritic conductances known to modulate the linearity of response summation (Cash and Yuste 1999; Larkum and Zhu 2002; Nettleton and Spain 2000; Schiller et al. 2000). Thus suppression may be a general feature of synaptic integration in cortical cells and not specific to sensory-evoked responses. To ascertain whether barrel cortex neurons and their local circuitry are capable of summating synaptic inputs without suppression, we used focal electrical stimulation of the cortex to evoke synaptic responses independent of sensory stimulation and characterized the integration of these events. If suppression results from nonspecific activation of dendritic conductances, we would expect integration of whisker- and electrically evoked synaptic

FIG. 10. Integration of electrically evoked synaptic responses. *A*: diagram of method for cortical electrical stimulation. Two bipolar stimulating electrodes (S1 and S2) were lowered into the cortex approximately 500–1,000 μm from the recording pipette. Stimulation intensity was adjusted to yield responses for which amplitude and fractional Rin were comparable to whisker-evoked responses. *B*: example of an RS cell at 972 μm depth. *Left histograms*: spike output (bin size = 5 ms). *Right traces*: average synaptic responses (n = 20 stimuli) at rest (−68 mV). Responses to stimulation of S1, S2, and S2 preceding S1 by 20 and 3 ms are shown. Triangles indicate times of electrical stimuli. Peak depolarization to S1 stimulation was increased at the 20-ms interval, although spike output was not changed. At the 30-ms interval, both the synaptic response and spike output were substantially increased. *C*: summary of spike and Vm response ratio values to S1 stimulation for the whole population. Response ratio was calculated as the magnitude of the S2–S1 response divided by the S1 response alone. Circles represent the value of this ratio for spike output on *left* (*Spikes*) and peak level of depolarization on *right* (*Vm*). Lines connect values from the same cell over the 2 S2–S1 intervals, 3 and 20 ms. Bars indicate the mean response ratios ± SD for each interval. Average response ratio was significantly >1 at the 3-ms interval for spikes and at both the 3- and 20-ms intervals for Vm. *D*: obtained value of S1-evoked PSP amplitude after S2 (c) at the 20-ms interval was plotted against the predicted S1-evoked PSP amplitude (a'). Data points were strongly correlated (r^2 = 0.78, solid line; $P < 0.001$), and the slope of the regression line did not differ significantly from unity.

responses to behave similarly. Figure 10*A* illustrates the experimental setup used for these experiments. Two bipolar stimulating electrodes were lowered about 1 mm into the cortex, with each located about 500–1,000 μm away from the recording pipette on opposite sides, a distance of about 2–4 barrels (Welker and Woolsey 1974). Electrical pulses (0.1-ms duration) of constant current were applied to the electrodes individually or sequentially, separated by intervals of 20 or 3 ms. Intensity of the stimuli was adjusted to yield responses with similar magnitude to those evoked by whisker deflection. Evoked responses in a representative RS cell (972 μm depth) are shown in Fig. 10*B*. Stimulation of electrode 1 (S1) evoked a suprathreshold response of 0.2 spikes per stimulus and a corresponding 6.6 mV PSP from a resting Vm of −68 mV. Stimulation of electrode 2 (S2) evoked a suprathreshold response of 0.3 spikes per stimulus and a corresponding PSP with an 8.6-mV amplitude and similar time course. When S2 preceded S1 by 20 ms, there was no change in the total spikes evoked by S1 (spike response ratio = 1.0), although the synaptic responses summed to give a peak depolarization from baseline of 10.6 mV (Vm response ratio = 1.6). When S2 preceded S1 by 3 ms, the spike output increase to 1.4 spikes per stimulus (spike response ratio = 7.0) and the resulting peak level of depolarization from baseline was 13.2 mV (Vm response ratio = 2.0).

We repeated this experiment in 10 cells. Electrically evoked PSPs were of similar amplitude, and caused similar reductions in Rin, as whisker deflections. Figure 10*C* illustrates the response ratios at 20- and 3-ms intervals for both the spike and PSP data. In contrast to the whisker data, at the 20-ms interval, the Vm response ratio was >1 in 8/10 cells (average response ratio = 1.25 ± 0.32; $P < 0.05$). At the same interval, the average spike response ratio (0.66 ± 0.46) did not differ significantly from 1. However, this value is strongly influenced by the 2 cells that showed modest reduction in the peak depolarization of the PW-evoked response but a total elimination of all suprathreshold responses, markedly reducing the average spike response ratio. At the 3-ms interval, 5/6 cells exhibited a spike response ratio >1 (average spike response ratio = 3.37 ± 2.2; $P < 0.05$) and 10/10 cells exhibited a Vm response ratio >1 (average Vm response ratio = 1.65 ± 0.40; $P < 0.05$).

We calculated the addition and multiplication components for the electrical stimulation data. Addition values were 0.24 ± 0.33 and 0.93 ± 0.49, and multiplication values were 1.01 ± 0.25 and 0.71 ± 0.39 for the 20- and 3-ms intervals, respectively. As with the whisker data, we also calculated the expected amplitude of the PW-evoked PSP given the preceding AW-evoked depolarization (see Fig. 5). In Fig. 10*D*, for the 20-ms interval, we plotted the observed PW-evoked PSP amplitude (c) against the expected value (a'). In contrast to the whisker data, the observed values were well predicted by the extrapolated values ($r^2 = 0.78$, solid line; $P < 0.001$). Furthermore, the slope of the regression line was not significantly different from unity ($P < 0.01$), strongly suggesting that the change in driving force is the principal explanation for the divisive amplitude reduction. Data for the 3-ms interval were similar (not shown).

We summarized the Vm response ratio results for the whisker (AW–PW 20 ms and AW–PW 3 ms) and electrical stimulation (S2–S1 20 ms and S2–S1 3 ms) data (Fig. 11*A*). We also compared the addition values and the ratios of observed to expected PSP amplitude (c/a') for the whisker and electrical stimulation experiments in Fig. 11, *B* and *C*. To compare current data with our published results, we also plotted the values for remote whisker–PW integration (RW–PW 20 ms; Higley and Contreras 2003).

Direct comparison of these groups illustrates 3 key findings. First, the Vm response ratios for the AW–PW and RW–PW interactions do not differ significantly at the 20-ms interval, nor do their addition and (c/a') values. This finding indicates that the underlying mechanisms of suppression described previously for remote whiskers (Higley and Contreras 2003) are phenomenologically similar to those underlying AW-mediated suppression.

Second, the response ratio for the AW–PW data are significantly smaller for the 20-ms interval than for the 3-ms interval, as is the addition component. In contrast, the (c/a') value does not differ between the 2 intervals. This result suggests that the mechanism underlying the amplitude reduction acts similarly at both 3- and 20-ms interdeflection intervals. Furthermore, the data demonstrate that the principal determinant of the magnitude of suppression in whisker–whisker interactions at these 2 intervals is the size of the addition component.

Third, the response ratio and (c/a') values are significantly smaller for the AW–PW interactions than for the electrical stimulation data at the same intervals. However, the addition components do not significantly differ. This finding argues that the principal mechanism underlying whisker-evoked suppression is the strong divisive reduction in PW-evoked response amplitude. Furthermore, because electrical stimulation and AW deflection evoked similar peak reductions in Rin (average fractional Rin: 0.78 ± 0.28 and 0.66 ± 0.25, respectively, not significantly different), the smaller AW–PW (c/a') values at both intervals argue against a postsynaptic conductance change as the mechanism underlying suppression.

One possible intracortical mechanism for suppression, consistent with disfacilitation, is a reduction in output of layer 4 neurons. To determine whether response integration at the 20-ms interval varied by layer, we compared the values of Vm response ratio with cortical depth for each cell (Fig. 11*D*). We classified cells as granular (Gr, 500–850 μm depth, $n = 8$), supragranular (SG, 0–500 μm depth, $n = 10$), or infragranular (IG, 850–1,800 μm depth, $n = 19$). The data from the present study are plotted as open squares with averages shown as filled squares and horizontally offset. Response ratio values from our previous study of remote whisker-mediated suppression are shown as open circles (filled circles indicate average). Vertical bars show the average response ratios for all cells (AW–PW and RW–PW data combined). The response ratios did not statistically differ between the 3 depth classifications, although the smallest values occurred predominantly within infragranular layers.

DISCUSSION

In an earlier study, we showed that PW response suppression by prior deflection of remote whiskers was predominantly a result of disfacilitation of the PW evoked excitation (Higley and Contreras 2003). In the present study, we attempted to

determine whether the same mechanisms underlie suppression by AW deflection and whether similar processes occur at a shorter, 3-ms interdeflection interval.

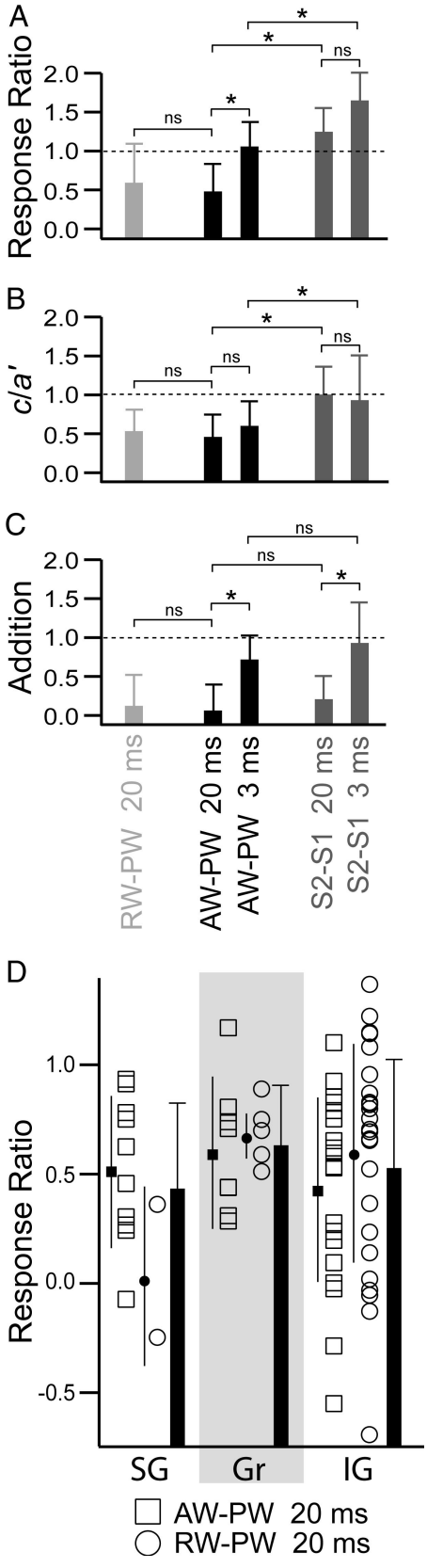

Consistent with previous studies (Higley and Contreras 2003; Wilent and Contreras 2004), the whisker-evoked PSPs consisted of an initial excitatory component followed by inhibition responsible for the large decrease in Rin and a longer-latency hyperpolarization. Compared with the PW-evoked response, the AW-evoked PSP was generally smaller in amplitude, occurred at longer onset latency, and exhibited a slower rate of rise compared with the PW-evoked response. Both PW and AW deflection caused comparable amounts of postsynaptic inhibition, as suggested by the similar reduction in the cell's Rin. As with our previous work on RW–PW interactions (Higley and Contreras 2003), the similarity of the PSP shape to PW and AW deflection within the same cell suggests that the PSP composition is largely determined by the local circuitry rather than the specific whisker deflected.

A potential source of disparity between our findings and those of previous studies is the current use of the anesthetic isoflurane. Isoflurane allowed us to maintain a more stable electroencephalographic state versus the repeated dosing of barbiturate necessary in our earlier study (Higley and Contreras 2003). A comparison of various PW-evoked response parameters indicated no significant difference between data collected under the two anesthetics. Nevertheless, subtle differences between the two anesthetic conditions may exist that we were unable to detect.

To study how the barrel system integrates converging inputs from the deflection of neighboring whiskers, we measured the response of cortical neurons to PW deflection when preceded either 20 or 3 ms by AW deflection. We quantified the interaction by calculating the ratio of the PW-evoked spike output when preceded by AW deflection to the spike output caused by PW deflection alone. Because the spike output of a cell is directly related to the underlying Vm, we also calculated the Vm response ratio of the peak level of PW-evoked depolarization from baseline when preceded by the AW to the peak level of depolarization from baseline arising from the PW alone. Thus a Vm response ratio <1 indicates that the peak Vm reached by the PW-evoked PSP in the combined response is hyperpolarized relative to control. We found that an AW–PW interval of 20 ms strongly suppressed the spike output of the cell and caused the PW-evoked PSP to reach a less-depolarized Vm in all cells. In contrast, when the AW–PW interval was reduced to 3 ms, the result was less consistent, yielding an average Vm response ratio that was significantly larger than that for the 20-ms interval.

Our data for the 20-ms interval are consistent with previous extracellular studies of AW–PW interactions (Simons 1985; Simons and Carvell 1989). However, our findings at the shorter

FIG. 11. Comparison of integration of whisker- and electrically evoked responses. *A*: average response ratios for AW–PW deflection (dark gray) and electrical stimulation (medium gray) at the 20- and 3-ms intervals. Data from remote-whisker (RW)–PW deflection (light gray) are shown from Higley and Contreras (2003) for comparison. Stars indicate a significant difference between bracketed groups (ns indicates no significant difference). *B*: average (*c*/*a*′) values plotted as for *A*. *C*: average addition values plotted as for *A*. *D*: plot of response ratio vs. cortical depth for AW–PW data (open squares) and RW–PW data [from Higley and Contreras (2003), open circles]. Cells were classified as supragranular (0–500 μm depth), granular (500–850 μm depth), or infragranular (850–1800 μm depth). Average values for AW–PW (filled square) and RW–PW (filled circle) data are shown for each depth category. Bars indicate average response ratios for AW–PW and RW–PW data combined. No significant differences between depth categories were found.

interval contrast somewhat with those of extracellular recordings by Shimegi et al. (1999), who observed significant supralinear summation of AW and PW spike responses when separated by intervals of 0–5 ms. This facilitation was observed in only 22% of all whisker pairings studied. In addition, analysis of single intervals (e.g., 3, 4, or 6 ms) revealed facilitation in <15% of supragranular and <5% of granular and infragranular cells (Shimegi et al. 1999; their Fig. 11). Therefore with our smaller population of intracellular recordings at the single 3-ms short interval, we may have failed to observe supralinear summation because of its low probability of occurrence.

Several mechanisms may explain the spike suppression and reduction in peak depolarization observed in the present study. Postsynaptic inhibition may reduce the response to PW-evoked excitation by 2 nonmutually exclusive processes. Hyperpolarizing inhibition occurs when negative currents linearly drive a cell's Vm away from spike threshold. Shunting inhibition occurs when an increased postsynaptic conductance divisively reduces the amplitude of subsequent synaptic potentials. Alternatively, AW response-mediated activation of dendritic outward currents (or deactivation of normally active inward currents) may oppose the electrotonic conduction of synaptic inputs to the soma. Finally, presynaptic reduction in excitatory input, either by synaptic depression or a simple decrease in presynaptic activity, could lead to a reduction in PW response.

Our data clearly demonstrate that the reduction in the peak Vm reached by the PW-evoked response at 20 ms is not the result of a hyperpolarizing PSP because the AW-evoked response is generally still depolarizing at that interval. Instead, there was a divisive reduction in the amplitude of the PW-evoked PSP. Although this reduction is consistent with shunting inhibition, 4 key findings argue against this possibility. *1*) There was no correlation between the reduction in Rin caused by AW deflection and the degree of divisive amplitude reduction after accounting for the effect of changes in driving force. *2*) The reduction in PW-evoked PSP amplitude did correlate with the reduction in dV/dt, a finding inconsistent with an increased conductance, which would expectedly decrease the cell's membrane time constant. *3*) AW deflection reduced the PW-evoked drop in Rin, also inconsistent with shunting, which would have expectedly increased the overall conductance of the cell. *4*) AW deflection also reduced the PW-evoked PSP amplitude even when the 2 had a similar Vrev, as for the cell in Fig. 8. In this case, the PW-evoked PSP reached a Vm further from the common apparent Vrev after AW deflection than when occurring alone. However, 2 conductances with the same Vrev should add to drive the Vm closer to that potential. This finding strongly indicates that the suppression cannot be explained by the preceding AW-evoked increase in conductance.

We found that an AW–PW interval of 3 ms also divisively reduced the PW-evoked PSP amplitude, although this reduction did not correlate with the change in Rin. Furthermore, the average value of the (c/a') did not differ significantly between the 20- and 3-ms intervals, whereas the magnitude of the addition component was significantly larger at the 3-ms interval. Thus the average lack of suppression at the shorter interval was attributed to the larger addition component caused by the closer temporal proximity of the PW response to the peak AW-evoked depolarization. Therefore we conclude that the interaction of whisker-evoked responses consistently involves a divisive reduction in PSP amplitude, but the determinant of the magnitude of suppression at differing interdeflection intervals is the size of the AW-evoked depolarization (the additive component).

Zhu and Zhu (2004) found that whisker deflection can evoke short latency synaptic responses in the distal apical dendrites of cortical pyramidal neurons. Furthermore, numerous groups have shown that certain subclasses of inhibitory interneurons make synapses on distal dendritic shafts and spines (Chu et al. 2003; Hestrin and Armstrong 1996; Tamas et al. 2003; Wang et al. 2004), suggesting that the interaction of synaptic events in the dendritic periphery may substantially impact sensory response integration. Because of the presumed somatic location of our recordings, we are unable to assess directly the contribution of distal inhibition to cross-whisker suppression. However, the finding that prior AW deflection at the 20-ms interval can reduce PW-evoked postsynaptic inhibition (see Figs. 8 and 9) argues against an exclusive role for distal inhibition.

Intrinsic properties of neurons strongly influence synaptic integration. Active potassium, sodium, and calcium conductances as well as voltage-dependent *N*-methyl-D-aspartate (NMDA) receptors can alter the linearity of summation of synaptic inputs (Cash and Yuste 1999; Larkum and Zhu 2002; Margulis and Tang 1998; Nettleton and Spain 2000; Schiller et al. 2000; Urban and Barrionuevo 1998). However, if nonspecific activation of these dendritic processes is responsible for the present findings, response suppression should be a general phenomenon that occurs for integration of any similar synaptic inputs. To evaluate the participation of such postsynaptic mechanisms independently of subcortical processes engaged by sensory stimulation, we quantified the summation of responses to direct electrical stimulation of the cortex. Our findings demonstrated that integration of two electrically evoked synaptic responses with amplitude, time course, and conductance changes similar to whisker-evoked responses resulted in an increase in both spike output and Vm response. Furthermore, the magnitude of the integrated synaptic response was well predicted as the linear sum of the individual components when we accounted for the change in driving force caused by the preceding PSP.

Two other findings argue against a strong role for active dendritic conductances in whisker response integration. First, the relationship of PSP amplitude to baseline Vm (see Fig. 5) was linear over the range of Vm values studied, suggesting that strong voltage-dependent dendritic conductances were not activated by the whisker stimuli used in the present study. Second, Larkum and Zhu (2002) found that dendritic spikes in vivo generally propagated to the soma where they elicited fast sodium potentials. However, we observed consistent PSP amplitude reduction in cells that failed to exhibit any suprathreshold response. In addition, we observed similar values of response suppression when cells were held at either resting or hyperpolarized Vm levels (data not shown). These findings suggest that inhibition of voltage-dependent dendritic action potentials is unlikely to explain cross-whisker suppression. Nevertheless, we cannot rule out a more subtle involvement of dendritic conductances, and further studies must address this possibility.

Our findings argue against a postsynaptic mechanism for AW-mediated suppression. This conclusion is in agreement

with our findings of RW–PW interactions and suggests a presynaptic mechanism. One possibility consistent with these findings is the withdrawal of input to the network, or disfacilitation. This conclusion is consistent with the finding that both excitation and inhibition are reduced at the 20-ms interval (see Fig. 9). Previously, we suggested that inhibition of recurrent activation of layer 4 neurons may reduce excitatory drive to supragranular and infragranular cells, leading to disfacilitation and suppression of the PW-evoked response throughout the barrel column (Higley and Contreras 2003). In the present study, a plot of response ratio against cell depth (see Fig. 11) showed no significant difference across layers, and the individual cases of strongest suppression typically occurred in infragranular neurons. Future studies are necessary to determine whether weak suppression in layer 4 can produce much stronger suppression in nongranular layers.

Another possible mechanism of disfacilitation may be depression of thalamocortical synapses, previously shown to undergo frequency adaptation at intervals $<$100 ms (Castro-Alamancos and Oldford 2002; Chung et al. 2002; Gibson et al. 1999; Gil et al. 1999). Whisker-responsive thalamic cells can exhibit suprathreshold receptive fields spanning multiple vibrissae (Diamond et al. 1992; Minnery et al. 2003; Simons and Carvell 1989; Timofeeva et al. 2004). Thus paired AW–PW deflections may possibly activate similar subpopulations of thalamocortical synapses that would depress at both 20- and 3-ms interdeflection intervals.

An intriguing alternative possibility is that suppression is mediated by GABAergic presynaptic inhibition of thalamocortical terminals. Previous studies have shown that activation of presynaptic $GABA_B$ receptors can inhibit glutamatergic transmission (Porter and Nieves 2004; Wu and Saggau 1995; Yamada et al. 1999). Furthermore, Porter and Nieves (2004) recently found that activation of $GABA_B$ receptors reduces thalamic excitation of neurons in the mouse barrel cortex. This possibility is consistent with our previous finding that the time course of cross-whisker suppression parallels that of the long-latency whisker-evoked hyperpolarization thought to be mediated by postsynaptic $GABA_B$ receptors (Higley and Contreras 2003).

Finally, previous studies have demonstrated that AW deflection can suppress PW responses in both the thalamus (Minnery et al. 2003; Simons and Carvell 1989) and trigeminal nucleus (Minnery et al. 2003), albeit less robustly than in the cortex. Again, it is presently unclear how the reduction in response magnitude at subcortical sites may correlate with cortical suppression. In conclusion, our findings indicate that prior AW deflection strongly reduces the amplitude of a subsequent PW-evoked PSP by reducing synaptic input to the cell. Furthermore, we propose that suppression involves synaptic integration at multiple points of multiwhisker response convergence in cortical and subcortical structures.

ACKNOWLEDGMENTS

The authors thank E. Garcia de Yebenes for the histology and J. A. Cardin, G. Civillico, N. Roy, and B. Wilent for helpful comments in preparation of this manuscript.

GRANTS

This work was sponsored by the Human Frontier Science Program Organization.

REFERENCES

Anderson JS, Carandini M, and Ferster D. Orientation tuning of input conductance, excitation, and inhibition in cat primary visual cortex. *J Neurophysiol* 84: 909–926, 2000.

Armstrong-James M and Fox K. Spatiotemporal convergence and divergence in the rat S1 "barrel" cortex. *J Comp Neurol* 263: 265–281, 1987.

Berger T, Larkum ME, and Luscher HR. High I(h) channel density in the distal apical dendrite of layer V pyramidal cells increases bidirectional attenuation of EPSPs. *J Neurophysiol* 85: 855–868, 2001.

Borg-Graham LJ, Monier C, and Fregnac Y. Visual input evokes transient and strong shunting inhibition in visual cortical neurons. *Nature* 393: 369–373, 1998.

Brecht M, Roth A, and Sakmann B. Dynamic receptive fields of reconstructed pyramidal cells in layers 3 and 2 of rat somatosensory cortex. *J Physiol* 2003.

Brecht M and Sakmann B. Dynamic representation of whisker deflection by synaptic potentials in spiny stellate and pyramidal cells in the barrels and septa of layer 4 rat somatosensory cortex. *J Physiol* 543: 49–70, 2002.

Bush PC and Sejnowski TJ. Effects of inhibition and dendritic saturation in simulated neocortical pyramidal cells. *J Neurophysiol* 71: 2183–2193, 1994.

Cash S and Yuste R. Linear summation of excitatory inputs by CA1 pyramidal neurons. *Neuron* 22: 383–394, 1999.

Castro-Alamancos MA and Oldford E. Cortical sensory suppression during arousal is due to the activity-dependent depression of thalamocortical synapses. *J Physiol* 541: 319–331, 2002.

Cauller LJ and Connors BW. Synaptic physiology of horizontal afferents to layer I in slices of rat SI neocortex. *J Neurosci* 14: 751–762, 1994.

Chapin JK. Laminar differences in sizes, shapes, and response profiles of cutaneous receptive fields in the rat SI cortex. *Exp Brain Res* 62: 549–559, 1986.

Chu Z, Galarreta M, and Hestrin S. Synaptic interactions of late-spiking neocortical neurons in layer 1. *J Neurosci* 23: 96–102, 2003.

Chung S, Li X, and Nelson SB. Short-term depression at thalamocortical synapses contributes to rapid adaptation of cortical sensory responses in vivo. *Neuron* 34: 437–446, 2002.

Connors BW and Gutnick MJ. Intrinsic firing patterns of diverse neocortical neurons. *Trends Neurosci* 13: 99–104, 1990.

Contreras D. Electrophysiological classes of neocortical neurons. *Neural Netw* 17: 633–646, 2004.

Coombs JS, Eccles JC, and Fatt P. Excitatory synaptic action in motoneurones. *J Physiol* 130: 374–395, 1955a.

Coombs JS, Eccles JC, and Fatt P. The inhibitory suppression of reflex discharges from motoneurones. *J Physiol* 130: 396–413, 1955b.

Diamond ME, Armstrong-James M, and Ebner FF. Somatic sensory responses in the rostral sector of the posterior group (POm) and in the ventral posterior medial nucleus (VPM) of the rat thalamus. *J Comp Neurol* 318: 462–476, 1992.

Dingledine R and Langmoen IA. Conductance changes and inhibitory actions of hippocampal recurrent IPSPs. *Brain Res* 185: 277–287, 1980.

Douglas RJ, Koch C, Mahowald M, Martin KA, and Suarez HH. Recurrent excitation in neocortical circuits. *Science* 269: 981–985, 1995.

Ghazanfar AA and Nicolelis MA. Nonlinear processing of tactile information in the thalamocortical loop. *J Neurophysiol* 78: 506–510, 1997.

Gibson JR, Beierlein M, and Connors BW. Two networks of electrically coupled inhibitory neurons in neocortex. *Nature* 402: 75–79, 1999.

Gil Z, Connors BW, and Amitai Y. Efficacy of thalamocortical and intracortical synaptic connections: quanta, innervation, and reliability. *Neuron* 23: 385–397, 1999.

Goldreich D, Kyriazi HT, and Simons DJ. Functional independence of layer IV barrels in rodent somatosensory cortex. *J Neurophysiol* 82: 1311–1316, 1999.

Hestrin S and Armstrong WE. Morphology and physiology of cortical neurons in layer I. *J Neurosci* 16: 5290–5300, 1996.

Higley MJ and Contreras D. Nonlinear integration of sensory responses in the rat barrel cortex: an intracellular study in vivo. *J Neurosci* 23: 10190–10200, 2003.

Hirsch JA, Alonso JM, Reid RC, and Martinez LM. Synaptic integration in striate cortical simple cells. *J Neurosci* 18: 9517–9528, 1998.

Holt GR and Koch C. Shunting inhibition does not have a divisive effect on firing rates. *Neural Comput* 9: 1001–1013, 1997.

Kawaguchi Y and Kubota Y. Correlation of physiological subgroupings of nonpyramidal cells with parvalbumin- and calbindinD28k-immunoreactive neurons in layer V of rat frontal cortex. *J Neurophysiol* 70: 387–396, 1993.

Kleinfeld D and Delaney KR. Distributed representation of vibrissa movement in the upper layers of somatosensory cortex revealed with voltage-sensitive dyes. *J Comp Neurol* 375: 89–108, 1996.

Koch C, Poggio T, and Torre V. Nonlinear interactions in a dendritic tree: localization, timing, and role in information processing. *Proc Natl Acad Sci USA* 80: 2799–2802, 1983.

Kuno M and Miyahara JT. Non-linear summation of unit synaptic potentials in spinal motoneurones of the cat. *J Physiol* 201: 465–477, 1969.

Kyriazi HT and Simons DJ. Thalamocortical response transformations in simulated whisker barrels. *J Neurosci* 13: 1601–1615, 1993.

Lang EJ and Pare D. Similar inhibitory processes dominate the responses of cat lateral amygdaloid projection neurons to their various afferents. *J Neurophysiol* 77: 341–352, 1997.

Lang EJ and Pare D. Synaptic responsiveness of interneurons of the cat lateral amygdaloid nucleus. *Neuroscience* 83: 877–889, 1998.

Langmoen IA and Andersen P. Summation of excitatory postsynaptic potentials in hippocampal pyramidal cells. *J Neurophysiol* 50: 1320–1329, 1983.

Larkum ME and Zhu JJ. Signaling of layer 1 and whisker-evoked Ca^{2+} and Na^{+} action potentials in distal and terminal dendrites of rat neocortical pyramidal neurons in vitro and in vivo. *J Neurosci* 22: 6991–7005, 2002.

Llinas R, Baker R, and Precht W. Blockage of inhibition by ammonium acetate action on chloride pump in cat trochlear motoneurons. *J Neurophysiol* 37: 522–532, 1974.

Llinas R and Terzuolo CA. Mechanisms of supraspinal actions upon spinal cord activities. Reticular inhibitory mechanisms on alpha-extensor motoneurons. *J Neurophysiol* 27: 579–591, 1964.

Margulis M and Tang CM. Temporal integration can readily switch between sublinear and supralinear summation. *J Neurophysiol* 79: 2809–2813, 1998.

Minnery BS, Bruno RM, and Simons DJ. Response transformation and receptive-field synthesis in the lemniscal trigeminothalamic circuit. *J Neurophysiol* 90: 1556–1570, 2003.

Mirabella G, Battiston S, and Diamond ME. Integration of multiple-whisker inputs in rat somatosensory cortex. *Cereb Cortex* 11: 164–170, 2001.

Monier C, Chavane F, Baudot P, Graham LJ, and Fregnac Y. Orientation and direction selectivity of synaptic inputs in visual cortical neurons: a diversity of combinations produces spike tuning. *Neuron* 37: 663–680, 2003.

Moore CI and Nelson SB. Spatio-temporal subthreshold receptive fields in the vibrissa representation of rat primary somatosensory cortex. *J Neurophysiol* 80: 2882–2892, 1998.

Moore CI, Nelson SB, and Sur M. Dynamics of neuronal processing in rat somatosensory cortex. *Trends Neurosci* 22: 513–520, 1999.

Nettleton JS and Spain WJ. Linear to supralinear summation of AMPA-mediated EPSPs in neocortical pyramidal neurons. *J Neurophysiol* 83: 3310–3322, 2000.

Porter JT and Nieves D. Presynaptic $GABA_B$ receptors modulate thalamic excitation of inhibitory and excitatory neurons in the mouse barrel cortex. *J Neurophysiol* 92: 2762–2770, 2004.

Sachdev RN, Sellien H, and Ebner FF. Direct inhibition evoked by whisker stimulation in somatic sensory (SI) barrel field cortex of the awake rat. *J Neurophysiol* 84: 1497–1504, 2000.

Schiller J, Major G, Koester HJ, and Schiller Y. NMDA spikes in basal dendrites of cortical pyramidal neurons. *Nature* 404: 285–289, 2000.

Shimegi S, Ichikawa T, Akasaki T, and Sato H. Temporal characteristics of response integration evoked by multiple whisker stimulations in the barrel cortex of rats. *J Neurosci* 19: 10164–10175, 1999.

Simons DJ. Response properties of vibrissa units in rat SI somatosensory neocortex. *J Neurophysiol* 41: 798–820, 1978.

Simons DJ. Multi-whisker stimulation and its effects on vibrissa units in rat SmI barrel cortex. *Brain Res* 276: 178–182, 1983.

Simons DJ. Temporal and spatial integration in the rat SI vibrissa cortex. *J Neurophysiol* 54: 615–635, 1985.

Simons DJ and Carvell GE. Thalamocortical response transformation in the rat vibrissa/barrel system. *J Neurophysiol* 61: 311–330, 1989.

Tamas G, Lorincz A, Simon A, and Szabadics J. Identified sources and targets of slow inhibition in the neocortex. *Science* 299: 1902–1905, 2003.

Timofeeva E, Lavallee P, Arsenault D, and Deschenes M. Synthesis of multiwhisker-receptive fields in subcortical stations of the vibrissa system. *J Neurophysiol* 91: 1510–1515, 2004.

Urban NN and Barrionuevo G. Active summation of excitatory postsynaptic potentials in hippocampal CA3 pyramidal neurons. *Proc Natl Acad Sci USA* 95: 11450–11455, 1998.

Wang Y, Toledo-Rodriguez M, Gupta A, Wu C, Luo J, Silberberg G, and Markram H. Anatomical, physiological and molecular properties of Martinotti cells in the somatosensory cortex of the juvenile rat. *J Physiol* 561: 65–90, 2004.

Welker C. Receptive fields of barrels in the somatosensory neocortex of the rat. *J Comp Neurol* 166: 173–189, 1976.

Welker C and Woolsey TA. Structure of layer IV in the somatosensory neocortex of the rat: description and comparison with the mouse. *J Comp Neurol* 158: 437–453, 1974.

Wilent WB and Contreras D. Synaptic responses to whisker deflections in rat barrel cortex as a function of cortical layer and stimulus intensity. *J Neurosci* 24: 3985–3998, 2004.

Woolsey TA and Van der Loos H. The structural organization of layer IV in the somatosensory region (SI) of mouse cerebral cortex. The description of a cortical field composed of discrete cytoarchitectonic units. *Brain Res* 17: 205–242, 1970.

Wu LG and Saggau P. GABAB receptor-mediated presynaptic inhibition in guinea-pig hippocampus is caused by reduction of presynaptic Ca^{2+} influx. *J Physiol* 485: 649–657, 1995.

Yamada J, Saitow F, Satake S, Kiyohara T, and Konishi S. GABA(B) receptor-mediated presynaptic inhibition of glutamatergic and GABAergic transmission in the basolateral amygdala. *Neuropharmacology* 38: 1743–1753, 1999.

Zhu JJ and Connors BW. Intrinsic firing patterns and whisker-evoked synaptic responses of neurons in the rat barrel cortex. *J Neurophysiol* 81: 1171–1183, 1999.

Zhu Y and Zhu JJ. Rapid arrival and integration of ascending sensory information in layer 1 nonpyramidal neurons and tuft dendrites of layer 5 pyramidal neurons of the neocortex. *J Neurosci* 24: 1272–1279, 2004.